Publications of the Astronomical Society of the Pacific
105: 308–314, 1993 March

The *R*- and Θ-Relief Method Applied to the Face-on Galaxy M51—Spoke and Ring Structures in the Nuclear Disk

YOSHIAKI SOFUE

Institute of Astronomy, University of Tokyo, Mitaka, Tokyo 181, Japan and Kiso Observatory, University of Tokyo, Kiso-gun, Nagano 397-01, Japan

Received 1992 November 10; accepted 1992 December 18

ABSTRACT. We propose a method of pattern recognition, called the *R*- and Θ-relief method, for studying fine structures in face-on galaxies, particularly in nuclear disks. This method enhances radial and azimuthal structures buried in a galactic disk. By applying the method to a *B*-band CCD image of face-on galaxy M51, we show that the nuclear disk is superposed by multiple rings and radial spoke structures. These peculiar features may be related to dynamical resonances and/or to an ejection activity near the nucleus. Amplitudes of *B*-band intensity of 100 pc scale structures are an order of magnitude greater in the central 1 kpc region than in the outer major arm regions, which indicates a much higher rate of star formation in the central regions than in arms.

1. INTRODUCTION

Optical images of spiral galaxies are characterized by their bright central bulges and outer spiral arms (e.g., Sandage 1961). CCD techniques have provided optical images with a high-dynamic range from the nucleus to the outer disk, which have revealed that, for example, the central regions of galaxies like M51 are full of clumpy as well as ring structures (Goad and Gallagher 1985; Pierce 1986). However, such structures have been not necessarily displayed correctly mainly because of the limited latitudes when printed: the difficulty in a morphological study of astrophysical structures contained in the images is the small dynamic range in displaying systems. In order to avoid such difficulty, some particular methods have been introduced as follows:

(a) *Relief method*: In this method, a spatially shifted image in a certain direction is subtracted from the original. This is a simple method to subtract a large-scale diffuse component, and is used to enhance compact objects like stars. This is convenient to distinguish faint stellar objects from faint nebulous objects or vice versa. We may call this method an X relief, where X is the axis of direction in which the original image is shifted.

(b) *Background filtering (BGF) technique (unsharp masking)*: The unsharp-masking method was applied to emulsion-device images, where an out-of-focused image is subtracted from the original. If the original data are in a digital format, images can be Gaussian-smoothed and subtracted from the original, and the residual image enhances small-scale structures. This method, called the BGF method, was developed in radio astronomy in order to subtract the background radio emission of the Milky Way and to enhance faint nebulous features (Sofue and Reich 1979). Recently this method has also been applied to CCD images (e.g., Fischer et al. 1990; Bridges and Hanes 1992). Alternatively, the images can be Fourier transformed and higher-order components are used to synthesize images in which fine structures are enhanced. This is often applied to interferometric data.

Although these methods do not add any information to the original data, one can study morphological structures in greater detail, which are detected in the original data but are embedded in bright foreground and background emission. Subtraction of diffuse and bright components with steep gradients is particularly useful when one wants to investigate morphological structures in the nuclear regions of galaxies, where brightness of the central bulge dominates over the disk components.

In this paper we propose a method, which we call the *R*- and Θ-relief method, in order to enhance features in the central regions of galaxies by taking into account the fact that galaxies are rotating around the nucleus.

2. *R*- AND Θ-RELIEF METHOD

Besides spiral arm structures in the outer disks of galaxies, various structures such as ring, bar, and oval structures in their central regions have been found, which are mostly a manifestation of dynamics and activity of the nuclear regions. An important aspect in tracing these structures is the fact that galaxies are rotating around their nuclei and galactic disks are more or less characterized by azimuthal and radial structures. Namely, structures in spiral galaxies may be best described in a r–θ coordinate systems, where r and θ are the radius and azimuthal angle, respectively.

The "*R*- and Θ-relief method," which we are proposing in this paper, has been developed for a purpose to investigate such structures in disk galaxies, particularly those in the nuclear regions. The method comprises of two parts, the R relief and Θ relief. The method can be operational using any software systems handling two-dimensional images. Here we use the standard IRAF package.

2.1 *R*-Relief Method

This *R*-relief method is introduced in order to enhance azimuthal features such as rings, oval structures, and small-pitch angle arms. On the other hand it looses (suppresses) information about radial features. The method is comprised of the following procedures: First the original image is MAGNIFied by a factor of μ, where μ depends on scales of structures in which we are interested, and is usually taken as 0.8–0.98. Then the magnified image is shifted by using IMSHIFT so that the image center coincides with the nucleus in the original image. Finally this magnified-and-shifted image is subtracted from the original by applying IMARITHmetic to get an *R*-relief image.

2.2 Θ-Relief Method

This method enhances radial structures such as spoke-like features and large-pitch angle arms, and is comprised of the following procedures, while it looses information about azimuthal structures. First the original image is shifted (IMSHIFT) so that the image center coincides with the nucleus. Then the image is rotated around the center (nucleus) using the ROTATE task by an angle θ. Again θ depends on the characteristic scale of interested features. Finally this rotated image is subtracted from the original, and we get a Θ-relief image.

If the galaxy to which the *R*- and Θ-relief method is applied is not face-on, it is required to rotate the image so that the major axis becomes horizontal (or vertical) and then to magnify in the minor-axis direction by a factor of sec i, where i is the inclination angle of the galaxy. In the following section we apply the *R*- and Θ-relief method to the face-on galaxy M51.

3. SPOKE-AND-RING STRUCTURE OF THE NUCLEAR DISK OF M51

We apply the method described in Sec. 2 to a *B*-band CCD image of M51.

3.1 Data for M51

The data we use here are those installed in the IRAF package as a standard test image (dev$pix). Figure 1 shows this image, which is the original to which the *R*- and Θ-relief method is applied. The image was taken 1987 April 5, at the KPNO 0.9-m telescope by Pat Seitzer (private communication). The detector was the KPNO TEK1 CCD, which has since been retired. The image has been transposed (columns to rows) so that north is up. The read noise for the chip was 8 electrons, and the gain was 3.2 electrons/ADU. TEK1 is a 512×512 device; raw data are taken with 32 overscan columns so that the raw framesize is 544×512 (columns $\times$ rows). It is finally trimmed to 508 $\times 508$. The MAGNIFY task was used to make the image with its current 512 square size. The pixel size is 0″.763, or 35.5 pc at a 9.6 Mpc distance of M51 ($1'' = 46.5$ pc).

3.2 BGF Image

Figure 2 shows the BGF image, where a smoothed image with the use of GAUSS task for a Gaussian beam of HPBW$=g=5$ pixels has been subtracted from the original. Besides the grand-design spiral pattern, there are various complicated features superposed on the spiral arms. We also notice the clumpy structures in the nuclear disk. Most of the knotty structures are clumpy star-forming regions and dark clouds.

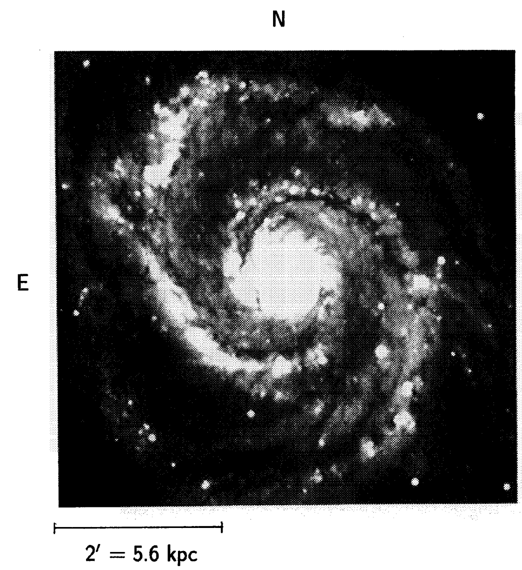

FIG. 1—Original *B*-band image of M51. See the text for the legend to the data. Top to the north, left to the east. The inset bar indicates $2' = 5.6$ kpc. (See Fig. 8 regarding intensity scale.)

3.3 *X*-Relief Image

Figure 3 is an image after applying the simple X relief with $\Delta X = 2$ pixels, where the X direction was chosen in the east–west direction. It is impressive that the nuclear disk is full of clumpy, bright knots, and is far more chaotic than in the outer spiral arm regions.

3.4 *R*-Relief Image

Figure 4 shows an *R*-relief image, where the magnifying factor was taken to be $\mu = 0.98$. Azimuthal and spiral features are enhanced. Note that the inner region is dominated by oval-ring structures.

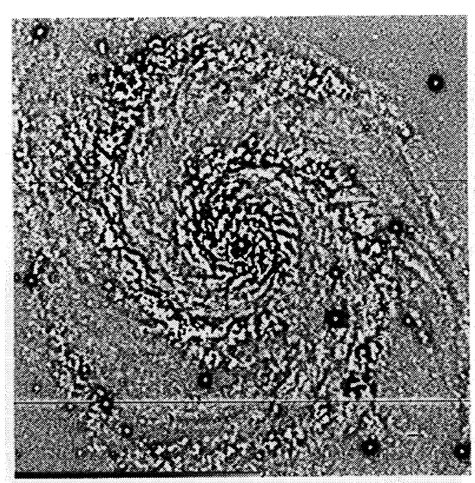

FIG. 2—BGF (background-filtered) image of M51 ($g=5$ pixels$=3''.82$). Same scale as Fig. 1. (See Fig. 8 regarding intensity scale.)

FIG. 3—X-relief image of M51 ($\Delta X=2$ pixels $=1''.53$). Same scale as Fig. 1. (See Fig. 8 regarding intensity scales.)

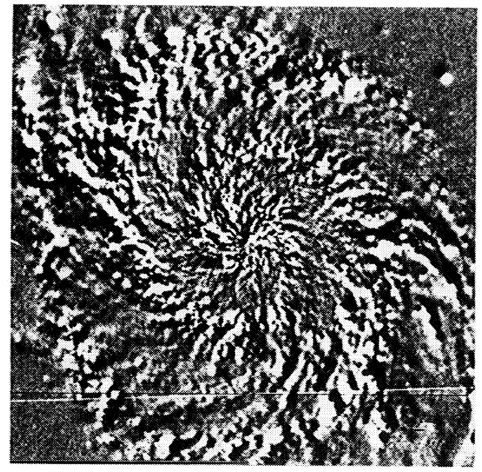

FIG. 5—Θ-relief image of M51 ($\theta=2°$). Same scale as Fig. 1. (See Fig. 9 regarding intensity scale.)

3.5 Θ-Relief Image

Figure 5 shows a Θ-relief image of M51, where θ was taken to be 2°. Numerous fine structures, which are either radial or with large-pitch angles, are found to be superposed on the grand-design spiral pattern. The radial and large-pitch angle patterns are evenly found in the interarm regions as well as in the central region. Also a remarkable fact is that the nuclear disk has a radial spoke-like pattern.

3.6 *R*-Relief Image of the Nuclear Disk

The R-relief image of the nuclear disk for $\mu=0.9$ is shown in Fig. 6, which enhances azimuthal structures. First of all, we notice the oval disk elongated in the direction of PA$=40°$, which has been noticed as a stellar oval by Pierce (1986). The direction of the major axis of this oval nuclear disk coincides with the direction of the bar of molecular gas (Nakai et al. 1991; Tosaki et al. 1991). The outer boundary of the oval disk is followed by dense spiral arms.

Most conspicuous in this display is the existence of multiple oval rings, which are elongated in the same direction as the oval disk mentioned above. The ring of radius 15″ ($=700$ pc) has been noticed on a $B-I$ image (Pierce 1986). However, a number of rings are found inside this ring, which were not detected (or recognized) by earlier analyses.

3.7 Θ-Relief Images of the Nuclear Disk

Figure 7 is the result of Θ-relief method applied to the central region of M51 with $\theta=10°$. The image is characterized by many coherent radial (or spoke-like) structures,

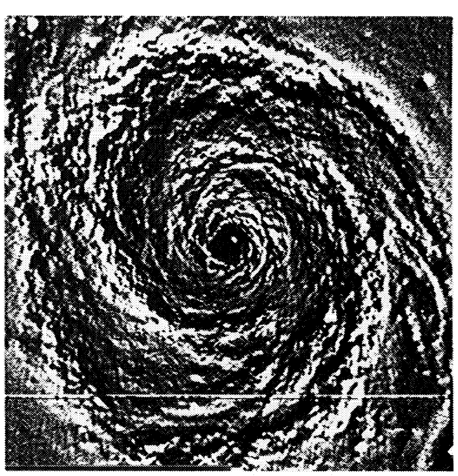

FIG. 4—R-relief image of M51 ($\mu=0.98$). Same scale as Fig. 1. (See Fig. 8 regarding intensity scale.)

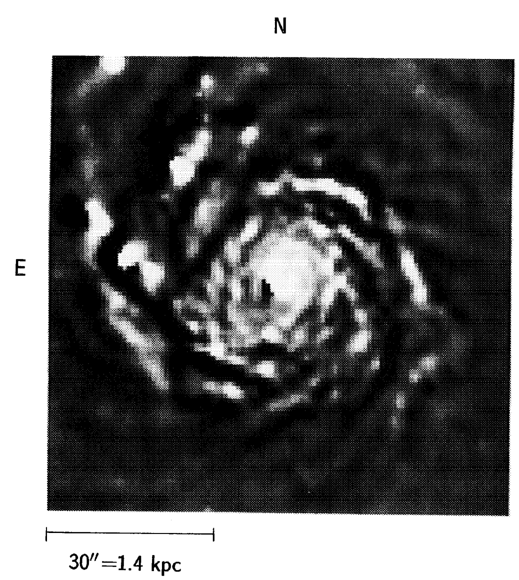

FIG. 6—R-relief image of the central region of M51 ($\mu=0.90$). The inset bar indicates $30''=1.4$ kpc. (See Fig. 8 regarding intensity scale.)

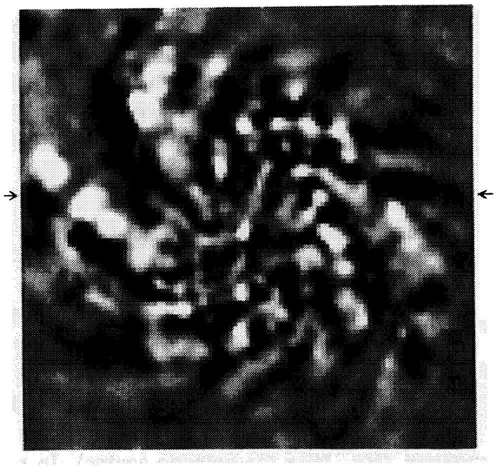

FIG. 7—Θ-relief image of the central region of M51 ($\theta=10°$). Same scale as Fig. 6. (See Fig. 9 regarding intensity scale.)

which are superposed on some noncoherent, random radial structures. Although random components may come from an artificial alignment effect of clumpy knots, the coherent "spokes," which are most evident in the northern region of the nuclear disk, are real structures. In fact the same features appear for different θ values within $2°<\theta<20°$. Moreover, the spoke-like feature becomes less evident, if the Θ relief is applied to an image with their image center offset from the nucleus. Hence, we may conclude that the coherently radial structure is a real feature associated with the nuclear region, but not due to an artificial effect through the reduction.

Spokes appear most clearly, when we take $\theta=5°$–$10°$, but become less clear for $\theta \lesssim 5°$ and for $>20°$. The contrast between the spoke and interspoke regions is much higher than that observed for the outer spiral arms (e.g., Fig. 4). A bright spoke runs through the nucleus from the southeast to the northwest at a position angle PA$=-40°$, and its position angle is coincident with the stellar oval and the molecular bar.

The spokes seem to stop at the end of the nuclear disk ($r\sim 20''=930$ pc), and there seems to exist a discontinuity between the spokes and outer spiral arms. The radial arms (spokes) start from the very nuclear region with large-pitch angles (almost $p\sim 90°$). Some of them stop at about 10–15″ (460–700 pc) from the nucleus, while some continue to the outer grand-designed, smaller-pitch-angle (about $p\sim 20°$) arms after a sudden change in their pitch angles at the edge of the nuclear disk at about 15″ (700 pc). In this context, the arms in and near the nuclear disk are similar to a barred-spiral galaxy, although many of the inner radial arms (spokes) seem to be independent of the outer arms.

3.8 Limitation and Variation of the *R*- and Θ-Relief Method

We comment on the limitation and problems of the *R*- and Θ-relief method. Since the method suppresses radial or azimuthal structures, it may happen that some accidentally radial or azimuthal (ring) features contained in random structures are enhanced. In fact, if one applies the method to an artificial exponential disk with noise, for example, radial or azimuthal (ring) features are enhanced to be shown up. This implies that we must be careful to judge if the structures are real or artifacts by examining the object from a more astrophysical point of view. Although the *R* and Θ coordinates are appropriate to represent structures in spiral galaxies, particularly features related to logarithmic spirals, they do not necessarily represent a physically meaningful distinction. Hence, the method may not be useful for discussion of more random and clumpy structures as those in amorphous galaxies.

The second problem is the fact that scale lengths of enhanced structures increase with the radius. On one hand, this is an advantage for discussion of such structures as related to logarithmic spirals as often observed for normal spiral galaxies. On the other hand, however, this is not good for discussion of such structures as star-forming regions and molecular clouds, which have rather constant or random correlation lengths of a few tens to a hundred pc, but do not necessarily increase with radius. Therefore, we should properly choose the values of θ and μ, depending on scale sizes and locations in which we are interested.

For the latter case, however, we could modify the *R*- and Θ-relief method as the following, although they are out of the standard IRAF tasks:

Constant ΔR relief: Instead of using the MAGNIFY task, the original image can be shifted in the radial direction by a constant pixel amount, say by ΔR. The radially shifted image is then subtracted from the original.

Constant ΔA relief: Instead of ROTATing the image, we shift individual pixels in the azimuthal direction by a constant amount, ΔA, where A is the azimuthal distance along an annulus. This can be done by changing the rotation angle θ with r proportional to $1/r$.

4. DISCUSSION

We have proposed an algorithm, called the *R*- and Θ-relief method, to enhance azimuthal and radial features, which are buried in bright bulge emissions of galaxies. Applying this method to the *B*-band CCD image of M51, we found various ring-and-radial spoke features superposed on the nuclear disk. In the following we discuss some implications of the obtained results. Here, however, we must keep in mind the limitations and problems of the method as pointed out in Sec. 3.8.

4.1 Nuclear Rings and Spokes

Implications of the $r=15''$ (700 pc) oval ring have been discussed in relation to the inner Lindblad resonance (e.g., Pierce 1986). However, the more inner oval rings are not explained within a simple scope of the resonance theory. They might be due to some corrugation effect excited by the major resonance. Alternatively they could be related to some nuclear activity such as expanding shock waves propagating through the nuclear disk, which are excited by multiple explosive events at the nucleus.

Implication of the radial spoke structure is not clear: there has been no theory to introduce such multiple radial spokes in the disk. Bright spokes are roughly parallel to the major axis of the oval ring, and could be due to the bar structure. In fact spokes running at PA$\sim$45° coincide roughly with the molecular bar showing a noncircular motion (Nakai et al. 1991; Tosaki et al. 1991), and could be a bar-shocked dark lane as found in barred-spiral galaxies.

An alternative possibility is that the spokes could be due to silhouettes produced by off-plane dust lanes flowing radially toward the halo from the nuclear region. Off-plane vertical filaments of dust lanes are seen in the central regions of active star-forming galaxies like M82 (Lynds and Sandage 1963) and NGC 253 (Sofue 1987). M51 is known to have ejection activity from the nucleus (Cecil and Rose 1984; Ford et al. 1985; Ho et al. 1987) and active star formation (Goad and Gallagher 1985). It would be possible that ejection takes place toward the halo, which accelerates dusty gaseous filaments in a similar manner to that occurring in M82 (Nakai et al. 1987). In fact a high-temperature gas flow has been suggested from X-ray observations (Palumbo et al. 1985), which might be associated with an outflow of molecular gas. If such off-plane filaments (dust lanes) exist in the nuclear region, they could produce radial silhouettes, when projected on the galaxy plane, and this may explain the spoke features.

4.2 Cross Sections of Relief Images

The reliefing techniques as described here, not only the R- and Θ-relief method but also the BGF (unsharp masking) and X-relief methods, are effective for pattern recognition of small-scale features buried in background emissions, particularly when the background emission has a steep gradient (e.g., near the galactic center). In particular, the R- and Θ-relief method is useful for abstracting coherently azimuthal and radial features, which are characteristic for such objects like disk galaxies usually described in an r–θ coordinate system. The methods also have the advantage that the results are not sensitive to large-scale inhomogeneities of baselevels in the original data. On the other hand, these methods seem to be not suitable for a quantitative analysis such as to derive lumi-

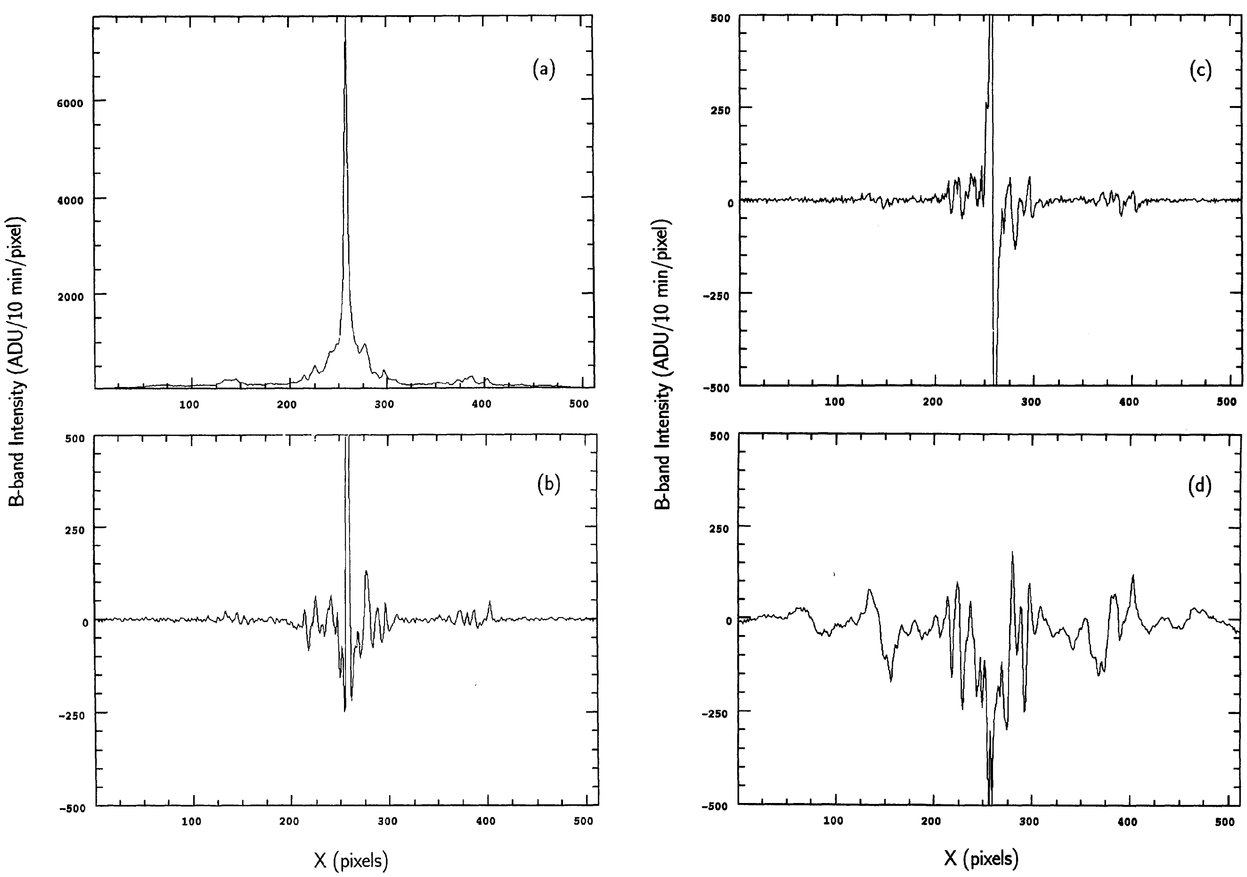

FIG. 8—East–west cross sections of intensity distribution across the nucleus. (a) original data in Fig. 1; (b) BGF image in Fig. 2 but for g=2 pixels=1.53″; (c) X-relief image in Fig. 3 (ΔX=2 pixels=1.53″); (d) R-relief image in Fig. 6 (μ=0.90). Intensity scale of 7750 units in the ordinate corresponds to the peak intensity of the nucleus (=NI), and the abscissa is in units of pixel numbers, where the entire 512 pixels correspond to 6.′5.

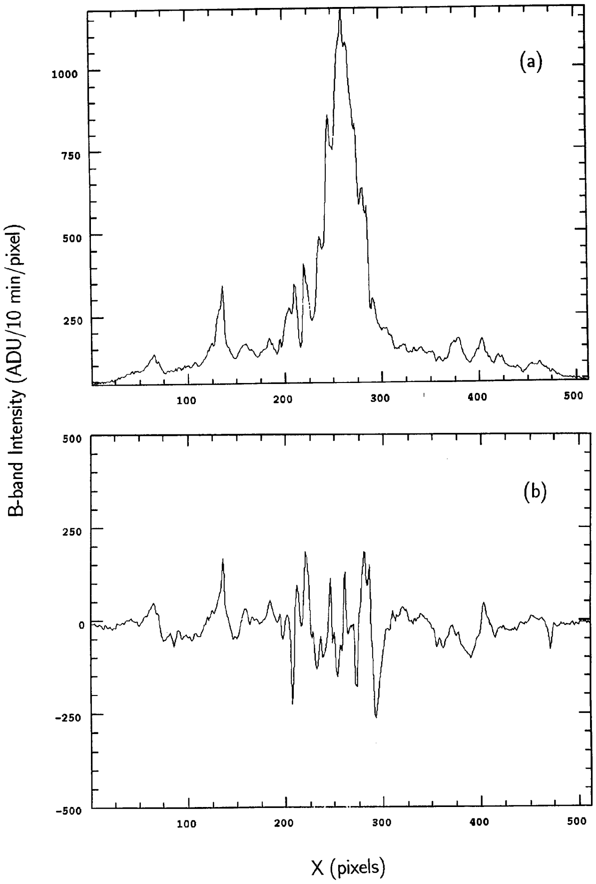

FIG. 9—East–west cross sections at 8″.4 north of the nucleus. (a) original data; (b) Θ-relief image in Fig. 7 ($\theta = 10°$: along the line indicated by arrows in Fig. 7). The ordinate and abscissa scales are the same as in Fig. 8.

nosities of abstracted features, since the methods display differential intensities and, as well, the results depend on the parameters μ and θ.

In order to get an impression about how the results can be used for a quantitative analyses, we compare cross sections of the obtained images. Figure 8 shows east–west cross sections of intensity distribution across the nucleus for (a) the original data in Fig. 1, (b) BGF image as Fig. 2 but for $g=2$ pixels, (c) *X*-relief image in Fig. 3 ($\Delta X=2$ pixels), and (d) *R*-relief image in Fig. 6 ($\mu=0.9$). The cross sections for the BGF and relief images [(b) to (d)] show almost the same characteristics.

Figure 9 shows east–west cross sections at 8″.4 north of the nucleus (along the line indicated by arrows in Fig. 7) for (a) the original data in Fig. 1 and (b) the Θ-relief image in Fig. 7 ($\theta=10°$). The radial spokes toward the north appear as the sharp peaks and valleys at pixel numbers 240–260 in Fig. 9(b), which are again hardly recognized in the original data [Fig. 9(a)]. However, from comparison of the cross sections for the relief and original data, we can confirm that the features appearing in the *R*- and Θ-relief images are real structures.

4.3 Increasing Star-Forming Rate toward the Nucleus

A significant fraction of the diffuse emission around the nucleus as seen in the original data [at $r<1$ kpc; Fig. 8(a)] may be due to a mixture of the bulge emission and the nuclear disk, which are not separated from each other. The diffuse emission amounts to about 6% to 10% of the intensity of the nucleus, which we hereafter denote as 0.06–0.10 NI (nucleus intensity). On the other hand, emission of about 0.01–0.03 NI from the small-scale features appearing in the relief images [Figs. 8(b) to 8(d)] is due to structures within the nuclear disk. Features of a few pixel scales are most effectively abstracted in the present reliefs, and they correspond to structures of 100 pc scale, which are typical for sizes of star-forming regions, interstellar molecular clouds, and the width of galactic shock waves.

It must be emphasized that the *B*-band intensities of 100 pc scale structures decreases with the distance from the nucleus, as is most clearly seen in Figs. 8(b) and 8(c). The intensities of the oval rings are of the order of 0.01–0.03 NI at $r<1$ kpc (e.g., 0.026 NI at the $15''=700$ pc ring). The innermost arm appearing at $r\sim\pm900$ pc has an intensity of about the same amount ($\sim$0.03 NI), and features appearing at $r\sim1$–2 kpc have less intensities of about 0.01 NI. Furthermore, outer features are $r\sim2$–3 kpc, which correspond to the major spiral arms, have intensities of about 0.005–0.006 NI.

From these facts we may conclude that the *B*-band intensities of 100 pc scale structures within the nuclear disk at $r=1$ to 2 kpc are an order of magnitude stronger than in the major spiral arms. Since the *B*-band intensity is deeply coupled with the star-forming regions such as OB associations and dark clouds (in silhouettes), this fact should indicate that the star-forming activity is much higher in the nuclear region than in the outer major arms. This is a natural consequence of the fact that an Sc Galaxy contains molecular gas whose density increases steeply toward the nucleus, as does the gas density in M51 (Nakai et al. 1991), and that the corresponding star-formation activity increases toward the nucleus.

This work was financially supported by the Ministry of Education, Science and Culture under Grant Nos. 01420001 and 01302009 (Y. Sofue). The author thanks Dr. K. Wakamatsu of Gifu University and Dr. T. Ichiwaka of the Kiso Observatory for their valuable discussions. He also thanks Dr. Pat Seitzer of KPNO for providing him with information about the IRAF demonstration image of M51, and Dr. Todd Boroson of NOAO for his critical reading of the manuscript and referee's invaluable comments.

REFERENCES

Bridges, T. J., and Hanes, D. A. 1992, AJ, 102, 800
Cecil, G., and Rose, J. A. 1984, ApJ, 287, 131
Fischer, P., Hesser, J. E., Harris, H. C., and Bothun, G. D. 1990, PASP, 102, 5
Ford, H. C., Crane, P. C., Jacoby, G. H., Lawrie, D. G., and van der Hulst, J. M. 1985, ApJ, 293, 132
Goad, J. W., and Gallagher III, J. S. 1985, ApJ, 297, 98

Ho, P. T., Martin, R. N., Henkel, C., and Turner, J. L. 1987, ApJ, 320, 663
Lynds, C. R., and Sandage, A. R. 1963, ApJ, 137, 1005
Nakai, N., Kuno, N., Handa, T., and Sofue, Y. 1991, in Dynamics of Galaxies and Their Molecular Cloud Distribution, ed. F. Combes and F. Casoli (Dordrecht, Kluwer), p. 63
Palumbo, G. G. C., Fabbiano, G., Fransson, C., and Trinchieri, G. 1985, ApJ, 298, 259
Pierce, M. J. 1986 AJ, 92, 285
Rots, A. H., Bosma, A., van der Hulst, J. M., Athanassoula, E., and Crane, P. C. 1990, AJ, 100, 387
Sofue, Y. 1987, PASJ, 39, 547
Tosaki, T., Kawabe, R., Ishiguro, M., Okumura, K., Morita, K. Kasuga, T., and Ishizuki, S. 1991, in Dynamics of Galaxies and Their Molecular Cloud Distributions, ed. F. Combes and F. Casoli (Dordrecht, Kluwer), p. 79